https://doi.org/10.48048/tis.2023.3766

A New Study on the Effect of Pure Anatase TiO_2 Film Thickness on Gentian Violet Photodegradation Under Sunlight: Considering the Effect of Hole Scavengers

Amer Mekkaoui, Elhachmi Guettaf Temam*, Saad Rahmane and Brahim Gasmi

Physics Laboratory of Thin Layers and Applications, University Mohamed Khider Biskra, Biskra 07000, Algeria

(*Corresponding author's e-mail: elhachemi.guettaf@univ-biskra.dz)

Received: 17 April 2022, Revised: 25 May 2022, Accepted: 1 June 2022, Published: 28 November 2022

Abstract

In this paper, pure anatase TiO_2 thin films were grown on glass substrates by using sol-gel dip-coating method. To study the physical, chemical and optical properties of the deposits, TiO_2 thin films were synthesized with thickness (241.5, 258.19, 230.33 and 302.35 nm). XRD patterns show that TiO_2 films were grown with unique anatase phase (101). The photocatalytic test shows that film (~ 302 nm) gives high photodegradation of gentian violet (GV) under sunlight irradiation due to the low number of defect sites. The increase in film thickness and the decrease of surface roughness and crystal size decrease the number of defect sites in the material which lead to low recombination rate of charge carriers. The use of Ag^+ as hole scavenger increases the photocatalytic activity 4.75 times within the first hour. The photocatalysis process showed that Ag+ can be reduced on the surface of photoactivated TiO_2 thin films to obtain sun-photodeposited/dip-coated AgO/TiO_2 (p-n) heterojunction.

Keywords: Dip-coating, Film thickness, TiO_2, Anatase, Gentian violet, Photocatalysis, Sun-photodeposition

Introduction

Technological and industrial development have contributed to many human life requirements; on the other hand, they have polluted the environment. Liquid industrial wastes containing dyes are thrown into the seas, rivers, and groundwater, which led to negative repercussions on human health. In recent years, several researches have been done on TiO_2 photocatalysis with the aim of developing methods to purify water [1-3]. Many investigations are mainly focused on TiO_2 material as photocatalysts for organic pollutants breakdown under ultraviolet [4-6] or sunlight irradiations [7-12]. The photocatalyst is inexpensive, readily available, non-toxic, chemically and mechanically stable.

The photocatalytic applications of TiO_2 are translation of their attractive properties such as high transmission in the visible region [13], cost-effectiveness, suitable valence band and conduction band positions, non-toxicity, strong oxidizing power and long-term stability. TiO_2 is an n-type semiconductor which can be crystallized in 3 different phases: anatase, brookite and rutile [14]. Rutile is the most stable phase than anatase and brookite [15]. Actually, the photocatalytic activity of TiO_2 is strongly dependent on its film thickness, phase structure, crystal size, and surface roughness and morphology. Rutile (3.0 eV) has higher absorbance ability under sun light than anatase (3.2 eV) due to tighter band gap. Anatase phase has a higher surface adsorption capacity to hydroxyl groups and a lower charge carrier recombination rate than rutile. Nanostructured TiO_2, particularly in the anatase form, exhibits photocatalytic activity under ultraviolet (UV) irradiation [16]. This photoactivity is reportedly most pronounced at the (001) planes of anatase [17].

However, the main factors that limit the photoactivity of pure anatase TiO_2 thin films are the rapid recombination of charge carriers (e^-/h^+) and the low roughness and porosity of the surface. Although the synthesis of rough TiO_2 thin films with porous structures and low crystallite size increase the number of surface sites for adsorption and breakdown of organic pollutants, it may raise the number of defect sites. The defect sites can trap the charge carriers which enhance the (e^-/h^+) recombination rate. This is a loss for photocatalysis process [2]. The number of defect sites can be reduced by several methods, namely,

increase film thickness, coupling with other semiconductors, doping and co-doping with metallic or nonmetallic ions [18-23].

In previous studies, the increase of film thickness has been proved to be a successful factor to improve the photoactivation of TiO_2 thin film. For example, Negishi *et al.* [24] studied the effect of TiO_2 films thickness by increasing number of dips and compared their photocatalytic activity for acetic acid under UV light with TiO_2 P-25 powder. They found that the photoactivity of TiO_2 films with high thickness (380 nm) is similar to that of P-25 powder. In other study, they disclosed that the photodecomposition of NO_x increases with the increase of TiO_2 film thickness to 1 µm [25].

In the literature, most studies were focused on TiO_2 content, deposition technique, annealing temperature, doping or co-doping with other metals [26-29], while the effect of film thickness on photoactivation properties of TiO_2 films is relatively few.

Herein, for the first time, the effect of film thickness on the photocatalytic activity of pure anatase TiO_2 films under sunlight irradiations has studied and explained. This work investigates the effect of film thickness on the structure, morphology, and optical properties of thin TiO_2 films dip-coated on glass substrates. It is found that 302 nm is an appropriate thickness for gentian violet (GV) high photodegradation under sunlight irradiations. Based on these findings, we have also studied the effect of Ag^+ and Glycerol as hole scavengers on the photocatalytic performance of TiO_2 thin films. The possibility of synthesizing sun-photodeposited/dipcoated (p-n) AgO/TiO_2 heterojunction has discussed for the first time.

Materials and methods

As a solvent, isopropanol and ethanol were used. Glacial acetic acid (GAA) was employed as a chelating agent. All experiments were performed with double distilled water (DW). Titanium (IV) isopropoxide ($Ti(OCH(CH_3)_2)_4$ was the precursor. As received from Sigma Aldrich, the chemical materials were used.

For the synthesis of TiO_2 thin films using the sol-gel dip coating method, 7 mL of titanium (IV) isopropoxide was dissolved in 10 mL of isopropanol. 4 mL of GAA was added dropwise to the sol with vigorous stirring. After 2 h, 29 mL of ethanol was added to give 50 mL of sol-gel and a dip-coated film of constant surface area (20 cm^2). The glass substrates were washed with boiling sulfuric acid solution (DW: H_2SO_4=1:10), then washed with DW and rinsed with acetone. Finally, rinse with distilled water. To obtain different film thickness, the substrates were soaked for different soaking times (30, 60, 90 and 120 s). The substrate was dipped and pulled out at a speed of 1 $mm.s^{-1}$, and dried at 100 °C for 10 min. This process was repeated 5 times to obtain a crystalline film. The thin TiO_2 films were calcined at 450 °C for 3 h with a heating rate of 5 °C/min using a muffle furnace. After cooling to room temperature, the produced films were further characterized.

GV dye is selected as a model for wastewater pollutants. The removal of GV using TiO_2 photocatalysts was investigated under sunlight exposure. The sample (20 cm^2) was immersed in 100 mL GV solution (2 ppm), protected from light for 2 h to reach the adsorption equilibrium, and the photodegradation test was carried out from 11:00 to 16:00. In these experiments, the GV solution was stirred at a constant speed (250 rpm). To improve the removal of GV, 0.1 M of both silver nitrate (Ag) and glycerol (Gl) were added to the contaminated solution as electron-hole scavengers. The samples used in this test were the ones that provided the best results without the use of electron-hole scavengers.

Results and discussion

The crystal structure of TiO_2 thin film is analyzed by XRD pattern as shown in **Figure 1**. All the films exhibit a tetragonal crystal structure with single anatase phase. No other phases were detected showing the purity of the produced samples. This is due to the fact that all the films were heated at the same temperature (450 °C) and the difference in film thickness between the lowest and the highest is not too great. It is evident that only one peak is observed at 25.4 ° corresponding to the (101) diffraction plane (JCPDS: 00-002-0387). The high intensity of the peaks indicates high crystallinity. Crystal size is one of the important factors influencing the photocatalytic activity of the material. The crystal size was estimated based on the effective crystal dimension D computed using Debye-Scherrer equation [30,31];

$$D = \frac{K.\lambda}{\beta.cos\theta} \quad (1)$$

where D is crystalline size, K is the Scherrer constant, λ is the incident wavelength of X- ray (1.5406 Å), β is the full width at half maximum intensity and θ is the diffraction angle. When the material grain size is small, the photocatalytic activity is very significant [32-34]. Table 1 indicates that films dip-coated at 120 s have the smallest crystal size (18.2 nm) which perhapspromise for high photocatalytic activity. All the films show low crystal size (D < 24 nm) confirming the nanostructure growth of the films.

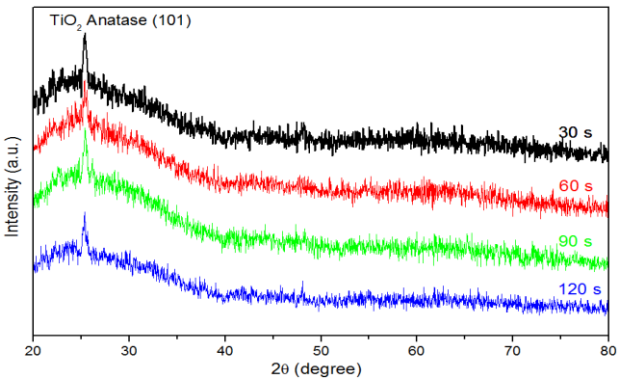

Figure 1 XRD patterns of TiO_2 based thin films.

The AFM micrographs of TiO_2 thin films are shown in **Figure 2**. The root mean square (Rq) surface roughness was calculated with the use of Apex analysis software (**Table 1**). The surface of TiO_2 thin films is heterogeneous. The maximum height of the films is 520 nm correspond to films synthesized at 30 s of dipping time. Rq is in the order of 25.9 > 12.6 > 11.8 > 10.5 nm corresponding to dipping time of 30 > 60 > 90 >120 s. The increase in surface roughness increases the specific surface area of the samples [35,36].

Table 1 Summary of analytical data.

Parameters	**Units**	**Dippings time (sec)**			
		30	**60**	**90**	**120**
Crystallographic Phase	-	anatase	anatase	anatase	anatase
Crystal Size	nm	23,1	19,2	23,5	18,2
Surface Roughness	nm	25.9	12.6	11.8	10.5
Film Thickness	nm	241.5	258.19	230.33	302.35
Transmission in Visible Range	%	~81	~81	~96	~98
Optical Indirect Band Gap	eV	3.26	3.28	3.5	3.55
Si Content	wt%	47.21	42.92	49.32	54.56
O Content	wt%	49.82	41.75	43.10	37.88
Ti Content	wt%	2.97	15.33	7.58	7.56
Photodegradation rate	%	~76	~80	~72	~84

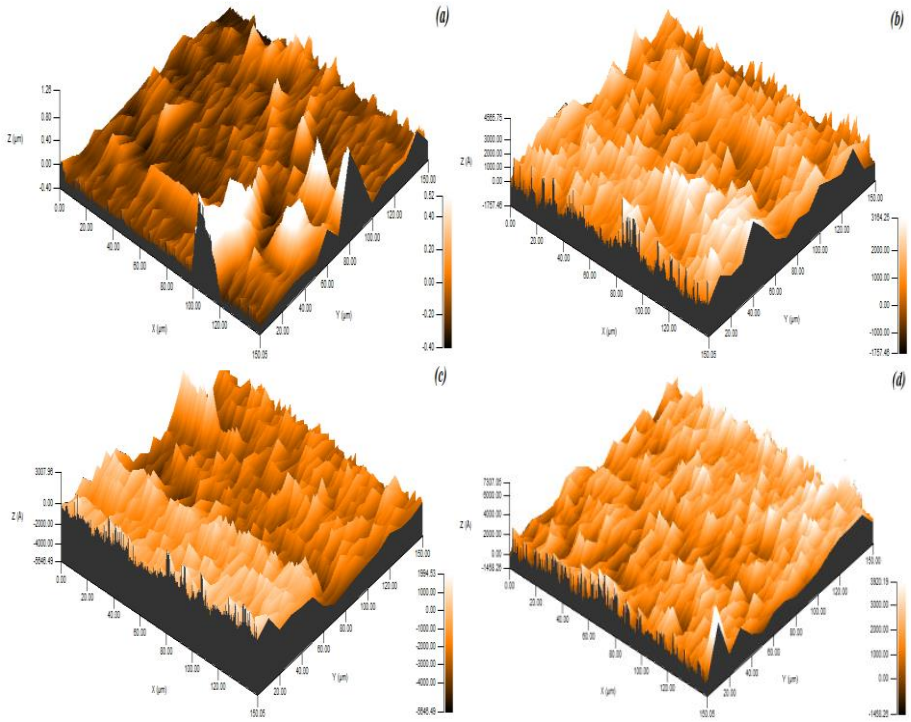

Figure 2AFM micrographs of TiO_2 thin films synthesized at different dipping time; (a) 30 s, (b) 60 s, (c) 90 s, and (d) 120 s.

SEM images of TiO_2 thin films are shown in **Figure 3**. The surface structure of the films is heterogeneous and fissured which enhances the specific surface area and results in high adsorption charge of dyes on the samples surfaces. Hence, the photocatalysis is significant. EDX analyses show a difference of the oxygen content in TiO_2 thin films as shown in **Figure 3**. As shown in **Table 1**, the oxygen content increases with the increase of film thickness. The increase in oxygen content in thin films increases its transmittance, and thus, giving high band gap energy (Eg) value [37]. The O content in TiO_2 thin films is in the range 37- 49 wt.% which leads to high transmittance in the visible range (**Table 1**). The thickness (t) of TiO_2 thin films was estimated by the gravimetric method using the relation;

$$t = \frac{M}{g.A} \quad (2)$$

Where t is the films thickness (nm), A is the surface area of the films (nm^2), M is the mass of the films (g), and g is the density of the film material ($g.nm^{-3}$) [38]. **Table 1** shows that films thickness increases by increasing dipping time. The films thickness is in the range of 241-302 nm.

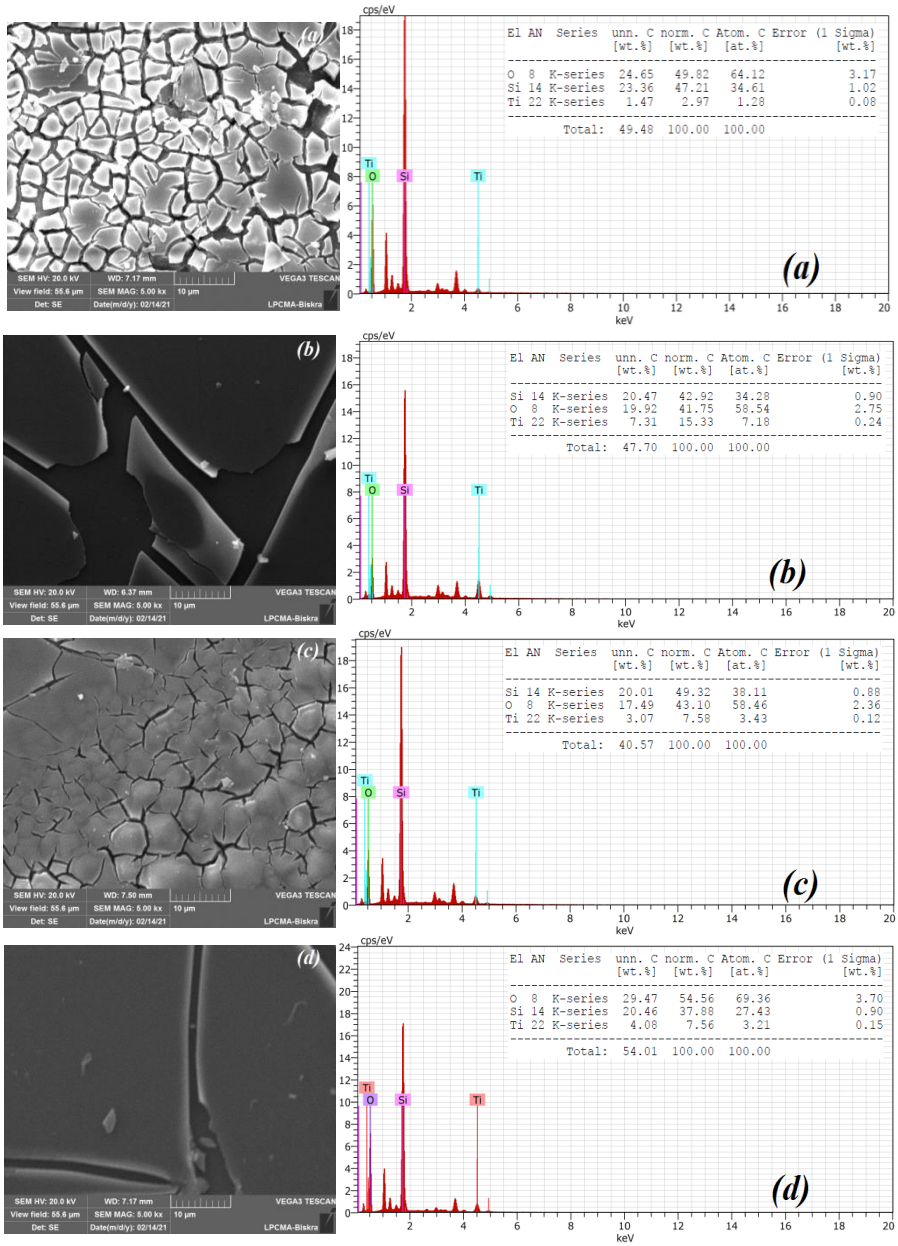

Figure3 SEM and EDX analyses of TiO_2 films produced at different dipping time; (a) 30 s, (b) 60 s, (c) 90 s, and (d) 120 s.

Figure 4 shows the optical transmission spectra of the films and Tauc plot for the optical band gap (Eg). The transmission spectra show high transparency in the visible region for all the TiO_2 thin films. These films have transmittance values greater than 80 %. The highest transmittance value is for TiO_2 with a high film thickness. It is tempting to conclude that the average transmittance is a function of film thickness (**Table1**). The optical indirect band gap was estimated using Tauc and Menth method given by relation Eqs. (3) and (4);

$$(\alpha h\nu)^{1/2} = C(h\nu - Eg) \quad (3)$$

$$\alpha = \frac{1}{t} ln(\frac{T}{100}) \quad (4)$$

where α is the absorption coefficient (m-1) (Eq. 4), that should be identified by the Eq. 4, h is Planck's constant ($4.136^{*}10^{-15}$eV.s), ν is Frequency of light (s^{-1}), C is a Constant, E_g is Optical indirect band gap (eV), t is the film thickness (m) and T is the optical transmittance (%) [39]. The band gap of the films is slightly increased with the increase of film thickness. Based on the literature [14,17], the anatase phase has a wide bandgap than in rutile and brookite phases, which suggestsas a high photocatalytic activity under constant photonic irradiation energy. This seems contradictory, whereas, the wider bandgap, the higher photonic energy required to migrate the electrons from valence to conductivity level.

$$E_C - E_V = E_g = E_A = E_0 \quad (5)$$

$$E_A > E_R > E_B \quad (6)$$

Where, E_C and E_V are conduction and valence level energy, respectively. E_g is the bandgap energy of the material. EA, ER and EB are the anatase, rutile and brookite bandgap energies. E_0 is the release factor (bandgap energy) that is defined as the energy required for electron migration. In order to stimulate an oxide material, the following condition must be met;

$$E_{ph} > E_0 \quad (7)$$

Where, E_{ph} is the photonic energy. From these 3 equations we can conclude that the wider bandgap the higher required activation photonic energy. Hence the recombination rate is low. Moreover, the higher photocatalytic activity of anatase phase than rutile and brookite phases is due to its low recombination rate as a stable electron and whole generation [40,41]. Zhang *et al.* [14] reported that indirect band gap anatase exhibits a longer life time of photoexcited electrons and holes than direct band gap rutile and brookite because the direct transitions of photogenerated electrons from the conduction band (CB) to valence band (VB) of anatase TiO_2 is impossible. Furthermore, anatase has the lightest average effective mass of photogenerated electrons and holes as compared to rutile and brookite [14].

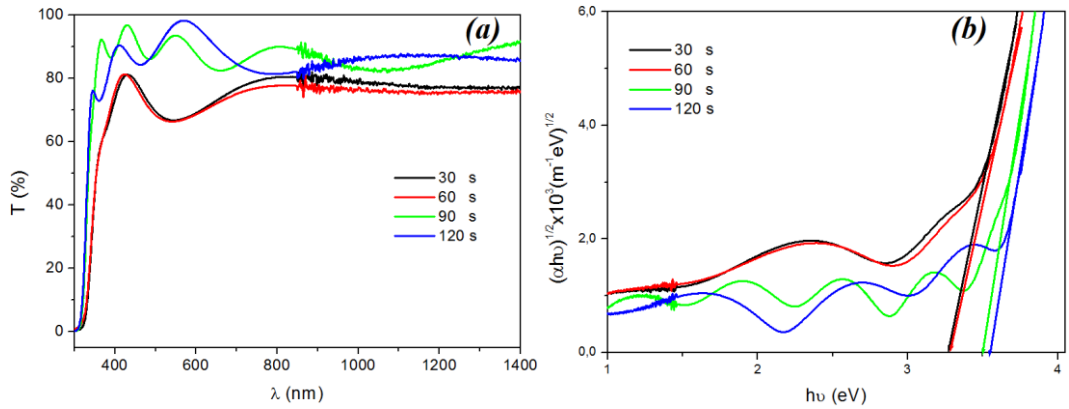

Figure 4(a) UV-VIS optical transmission spectra of TiO_2 thin films, (b) Tauc plot for the optical band gap.

The photocatalytic activity of TiO_2 thin films was evaluated through the photodegradation of GV (2 ppm) in an aqueous solution under sunlight irradiation. **Figure 5(a)** shows that GV decomposes continuously throughout the entire irradiation time. The rate of degradation varies according to the hour of irradiation. The photocatalytic efficiency (γ) is determined from the following equation;

$$\gamma\% = \frac{A_0 - A_t}{A_0} \quad (8)$$

where, A_0 and A_t are the absorbance at 582 nm of GV at t = 0 and t h, respectively. The degree of GV degradation is in the order 84 > 80 > 76 > 72 % corresponding to 120 > 60 > 30 > 90 s of dipping time as shown in **Figure 5(b)**. All the films show high photocatalytic activity that varies based on the dip

duration, which affects the thickness of the film. Overall, the best solar photocatalyst corresponds to the longer dip duration. **Figure 5(c)** shows that the photodegradation rate of GV is strongly depended on the film thickness. This finding confirmed several previous literary studies [24,25]. A thorough analysis of this process is required to understand the effect of film thickness on photocatalytic activity. Under solar irradiation, electron-hole pairs are generated and initiate the migration of charge carriers to the film surface, thereby, triggering the redox reactions of GV breakdown. Defect sites found in TiO_2 films can trap these charge carriers and increase their recombination. Hence, the GV decomposition process is reduced. The defect sites are ones of the most important factors affecting the recombination of charge carriers, and thus, affecting the breakdown of organic pollutants [2]. In turn, the number of defect sites is strongly depended on film thickness, grain refinements and surface roughness. Increasing in film thickness, decreasing in surface roughness and refinement of crystal size reduce the number of defect sites and then enhance the concentration of charge carriers on the surface of the materials. The film dip-coated at 120 s has the lowest crystal size and surface roughness and the highest thickness.

Figure 5(d) shows the degradation rate of GV in the presence of Ag^+ and Glycerol as hole-scavengers. We observe that the presence of Glycerol decreases the photodegradation of GV although it has shown significant results in several other literary studies [42,43]. The addition of glycerol increases the solubility of GV in water, thereby, inhibiting the adsorption equilibrium. The photodegradation rate in the presence of Ag+ achieves 95 % in the first hour which increases the decomposition of GV for 4.75 times. Unintentionally, we observed another phenomenon. The color of the sample is dark gray, indicating that silver has been deposited on the titanium oxide film (Eq.10). This process called solar photodeposition that produces a (p-n) heterojunction AgO/TiO_2 films after annealing in the atmosphere or under oxygen-supplied conditions. This process has 2 objectives in so-called killing 2 birds with 1 stone. The first is to purify water from silver metal; the second is to produce heterojunction AgO/TiO_2 film. We look forward to the experience of photodeposited/dip-coated AgO/TiO_2 films and study their properties in the upcoming works. The photodeposition of Ag metal on sun-photoactivated TiO_2 films is summarized by Eqs. (9) and (10);

$$TiO_2 \xrightarrow{hv} TiO_2\left(\frac{e^-}{h^+}\right) \longrightarrow e_{CB}^- + h_{VB}^+ \quad (9)$$

$$e_{CB}^- + Ag^+ \longrightarrow Ag \quad (10)$$

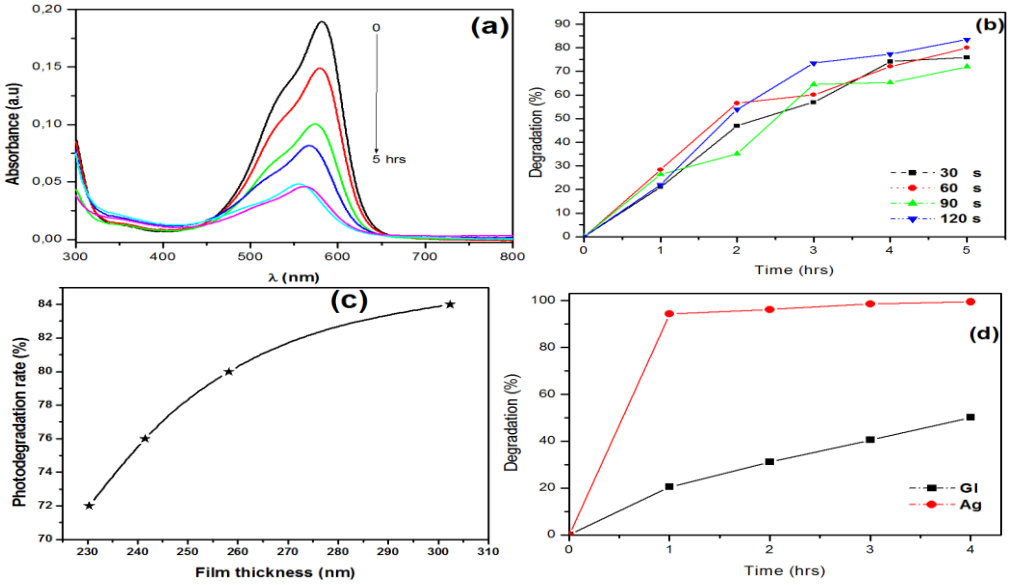

Figure 5(a) Variation of UV-vis spectra of GV during photodegradation over TiO_2 thin films; (b) Plot of photocatalytic efficiency versus the irradiation time; (c) plot of film thickness versus photodegradation rate; (d) Degradation rate in the presence of hole-scavengers.

Conclusions

In this paper, the photocatalytic properties nanostructured pure anatase TiO_2 thin films synthesized via sol-gel dip-coating method which were investigated via the photodegradation of GV under sunlight irradiations. The effect of film thickness on the photocatalytic activity was discussed in depth. Structural and surface analysis showed that the crystal size and surface roughness decreased with increasing dipping time. The SEM images show that rough and fissured surface morphology can enhance the adsorption of GV on the surface of TiO_2 films. All films showed high transmittance in the visible range. It has been found that increasing the dipping time increases the film thickness; and thus, having the opportunity to reduce the number of defect sites in the TiO_2 film. Therefore, the recombination rate is low. Using Ag^+ as a hole scavenger increases the photocatalytic activity 4.75 times within the first hour. We must point out that another phenomenon has occurred, namely, the reduction of silver ions on the surface of sun-photoactivated TiO_2 films, resulting in sun-photodeposited/dip-coated AgO/TiO_2 (p-n) heterojunction.

Acknowledgements

The authors declare that they have no known competing financial interests or personal relationships that could have appeared to influence the work reported in this paper.

References

[1] S Obregón and V Rodríguez-González. Photocatalytic TiO_2 thin films and coatings prepared by sol–gel processing: a brief review. *J. Sol Gel Sci. Tech*. 2021; **102**, 125-41.

[2] K Eufinger, D Poelman, H Poelman, RDGryse and GB Marin. *TiO_2 thin films for photocatalytic applications*. *In*: S Nam (Ed.). Thin solid films: Process and applications. Transworld Research Network, Kerala, India, 2008, p. 189-227.

[3] K Sunada, Y Kikuchi, K Hashimoto and A Fujishima. Bactericidal and detoxification effects of TiO_2 thin film photocatalysts. *Environ. Sci. Tech.* 1998; **32**, 726-8

[4] B Hao, J Guo, L Zhang and H Ma. Magnetron sputtered TiO_2/CuO heterojunction thin films for efficient photocatalysis of Rhodamine B. *J. Alloy. Comp*. 2022; **903**, 163851.

[5] I Levchuk, T Homola, G Singhal, JJ Rueda-Márquez, J Vida, P Souček, T Svoboda, E Villar-Navarro, O Levchuk, P Dzik, A Lähde and J Moreno-Andrés. UVA and solar driven photocatalysis with rGO/TiO_2/polysiloxane for inactivation of pathogens in recirculation aquaculture systems (RAS) streams. *Chem. Eng. J. Adv*. 2022; **10**, 100243.

[6] CB Anucha, I Altin, E Bacaksiz and VN Stathopoulos. Titanium dioxide (TiO_2)-based photocatalyst materials activity enhancement for contaminants of emerging concern (CECs) degradation: In the light of modification strategies. *Chem. Eng. J. Adv*. 2022; **10**, 100262.

[7] YM Hunge, MA Mahadik, AV Moholkar and CH Bhosale. Photoelectrocatalytic degradation of oxalic acid using WO_3 and stratified WO_3/TiO_2 photocatalysts under sunlight illumination. *Ultrason. Sonochem.* 2017; **35**, 233-42.

[8] YM Hunge. Sunlight assisted photoelectrocatalytic degradation of benzoic acid using stratified WO_3/TiO_2 thin films. *Ceram. Int.* 2017; **43**, 10089-96.

[9] A Lee, JA Libera, RZ Waldman, A Ahmed, JR Avila, JW Elam and SB Darling. Conformal Nitrogen-Doped TiO_2 Photocatalytic Coatings for Sunlight-Activated Membranes. *Adv. Sustain. Syst.* 2017; **1**, 1600041.

[10] I Barba-Nieto, U Caudillo-Flores, M Fernández-García and Anna Kubacka. Sunlight-operated TiO_2-based photocatalysts. *Molecules* 2020; **25**, 4008.

[11] DA Solís-Casados, L Escobar-Alarcón, V Alvarado-Pérez and E Haro-Poniatowski. Photocatalytic activity under simulated sunlight of Bi-modified TiO_2 thin films obtained by sol gel. *Int. J. Photoenergy* 2018; **2018**, 8715987.

[12] Y Zhiyong, H Keppner, D Laub, E Mielczarski, J Mielczarski, L Kiwi-Minsker, A Renken and J Kiwi. Photocatalytic discoloration of methyl orange on innovative parylene-TiO_2 flexible thin films under simulated sunlight. *Appl. Catal. B Environ.* 2008; **79**, 63-71.

[13] YM Evtushenko, SV Romashkin, NS Trofimov and TK Chekhlova. Optical properties of TiO_2thin films. *Phys. Procedia* 2015; **73**, 100-7.

[14] J Zhang, P Zhou, J Liu and J Yu. New understanding of the difference of photocatalytic activity among anatase, rutile and brookite TiO_2. *Phys. Chem. Chem. Phys*. 2014; **16**, 20382-6.

[15] AM Alotaibi, BAD Williamson, S Sathasivam, A Kafizas, M Alqahtani, C Sotelo-Vazquez, J Buckeridge, J Wu, SP Nair, DO Scanlon and IP Parkin. Enhanced photocatalytic and antibacterial ability of cu-doped anatase TiO_2thin films: Theory and experiment. *ACS Appl. Mater. Interfac.* 2020; **12**, 15348-61

[16] S Tanemura, L Miao, W Wunderlich, M Tanemura, Y Mori, S Toh and K Kaneko. Fabrication and characterization of anatase/rutile-TiO_2 thin films by magnetron sputtering: A review. *Sci. Tech. Adv. Mater*. 2005; **6**, 11-7.

[17] L Chu, Z Qin, J Yang and X Li. Anatase TiO_2nanoparticles with exposed {001} facets for efficient dye-sensitized solar cells. *Sci. Rep*. 2015; **5**, 12143.

[18] D Komaraiah, E Radha, J Sivakumar, MV Ramana Reddy and R Sayanna. Photoluminescence and photocatalytic activity of spin coated Ag^+ doped anatase TiO_2 thin films. *Opt. Mater.* 2020; **108**, 110401.

[19] M Behpour, R Foulady-Dehaghi and N Mir. Considering photocatalytic activity of N/F/S-doped TiO_2 thin films in degradation of textile waste under visible and sunlight irradiation. *Sol. Energ*. 2017; **158**, 636-43.

[20] S Parmar, T Das, B Ray, B Debnath, S Gosavi, GS Shanker, S Datar, S Chakraborty and S Ogale. N, H dual-doped black anatase TiO2 thin films toward significant self-activation in electrocatalytic hydrogen evolution reaction in alkaline media. *Adv. Energ. Sustain. Res*. 2022; **3**, 2100137.

[21] O Beldjebli, R Bensaha and P Panneerselvam. Effect of both sn doping asnd annealing temperature on the properties of dip-coated nanostructured TiO_2thin films. *J. Inorg. Organomet. Polymer. Mater*. 2022, **32**, 1624-36.

[22] SV Singh, U Gupta, S Biring, B Mukherjee and BN Pal. In-situ grown nanoscale p-n heterojuction of Cu_2S-TiO_2 thin film for efficient photoelectrocatalytic H_2 evolution. *Surface. Interfac.* 2022; **28**, 101660.

[23] D Tekin, H Kiziltas and H Ungan. Kinetic evaluation of ZnO/TiO_2 thin film photocatalyst in photocatalytic degradation of Orange G. *J. Mol. Liq.* 2020; **306**, 112905.

[24] N Negishi, T Iyoda, K Hashimoto and A Fujishima. Preparation of transparent TiO_2thin film photocatalyst and its photocatalytic activity. *Chem. Lett*. 1995; **24**, 841-2.

[25] N Negishi, K Takeuchi and T Ibusuki. Surface structure of the TiO_2 thin film photocatalyst. *J. Mater. Sci*. 1998; **33**, 5789-94.

[26] RS Sonawane and MK Dongare. Sol-gel synthesis of Au/TiO_2 thin films for photocatalytic degradation of phenol in sunlight. *J. Mol. Catal. Chem.* 2006; **243**, 68-76.

[27] B Karunagaran, P Uthirakumar, SJ Chung, S Velumani and EK Suh. TiO_2 thin film gas sensor for monitoring ammonia. *Mater. Char.* 2007; **58**, 680-4.

[28] T Wen, J Gao, J Shen and Z Zhou. Preparation and characterization of TiO_2 thin films by the sol-gel process, *J. Mater. Sci*. 2001; **36**, 5923-6.

[29] DE Yıldız, HH Gullu and HK Cavus. Effect of TiO_2thin film with different dopants in bringing au-metal into a contact with n-Si. *J. Inorg. Organomet. Polym. Mater.*2022; **32**, 1-11.

[30] DR Sarker, MN Uddin, M Elias, Z Rahman, RK Paul, IA Siddiquey, MA Hasnat, R Karim, MA Arafath and J Uddin. P-doped TiO_2-MWCNTs nanocomposite thin films with enhanced photocatalytic activity under visible light exposure. *Cleaner Eng. Tech*. 2022; **6**, 100364.

[31] E Radha, D Komaraiah, R Sayanna and J Sivakumar. Photoluminescence and photocatalytic activity of rare earth ions doped anatase TiO_2 thin films. *J. Lumin.* 2022; **244**, 118727.

[32] K Eufinger, D Poelman, H Poelman, RDGryse and GB Marin. Effect of microstructure and crystallinity on the photocatalytic activity of TiO_2 thin films deposited by dc magnetron sputtering. *J. Phys. Appl. Phys.* 2007; **40**, 5232.

[33] S Iti Kitazawa, Y Choi, S Yamamoto and T Yamaki. Rutile and anatase mixed crystal TiO_2 thin films prepared by pulsed laser deposition. *Thin Solid Films* 2006; **515**, 1901-4.

[34] Z Zarhri, MÁA Cardos, Y Ziat, M Hammi, OE Rhazouani, JCCArgüello and DA Avellaneda. Synthesis, structural and crystal size effect on the optical properties of sprayed TiO_2 thin films: Experiment and DFT TB-mbj. *J. Alloy. Comp.* 2020; **819**, 153010.

[35] MI Mendoza-Diaz, A Lecestre, L Salvagnac, B Bounor, D Pech, M Djafari-Rouhani, A Esteve and C Rossi. High surface area TiO_2 photocatalyst for H_2 production through silicon micromachining. *Appl. Surf. Sci*. 2022; **588**, 152919.

[36] ZS Hosseini, F Haghparast, AA Masoudi and A Mortezaali. Enhanced visible photocatalytic performance of un-doped TiO_2 nanoparticles thin films through modifying the substrate surface roughness. *Mater. Chem. Phys*. 2022; **279**, 125530.

[37] E Jimenez-Relinque and M Castellote. Hydroxyl radical and free and shallowly trapped electron generation and electron/hole recombination rates in TiO_2 photocatalysis using different combinations of anatase and rutile. *Appl. Catal. Gen.* 2018; **565**, 20-5.
[38] A Abdelkrim, S Rahmane, O Abdelouahab, A Hafida and K Nabila. Optoelectronic properties of SnO_2 thin films sprayed at different deposition times. *Chin. Phys. B* 2016; **25**, 046801.
[39] J Tauc and A Menth. States in the gap. *J. Non Crystalline Solid.* 1972; **8-10**, 569-85.
[40] DAH Hanaor and CC Sorrell. Review of the anatase to rutile phase transformation. *J. Mater. Sci*. 2011; **46**, 855-74.
[41] A Sclafani and JM Herrmann. Comparison of the photoelectronic and photocatalytic activities of various anatase and rutile forms of titania in pure liquid organic phases and in aqueous solutions. *J. Phys. Chem.* 1996; **100**, 13655-61.
[42] M Ibadurrohman and K Hellgardt. Photoelectrochemical performance of graphene-modified TiO_2 photoanodes in the presence of glycerol as a hole scavenger. *Int. J. Hydrogen Energ*. 2014; **39**, 18204-15.
[43] Y Wang, H Wang, Y Yang and B Xin. Magnetic $NiFe_2O_4$ 3D nanosphere photocatalyst: Glycerol-assisted microwave solvothermal synthesis and photocatalytic activity under microwave electrodeless discharge lamp. *Ceram. Int.* 2021; **47**, 14594-602.